JOURNAL OF SOLID STATE CHEMISTRY 28, 185–193 (1979)

Elastic and Inelastic Neutron Studies of Hydrogen Molybdenum Bronzes

P. G. DICKENS AND J. J. BIRTILL

Inorganic Chemistry Laboratory, Oxford

AND C. J. WRIGHT

A.E.R.E., Harwell, Didcot, Oxon, United Kingdom

Received January 30, 1978; in revised form July 31, 1978

Hydrogen molybdenum bronzes H_xMoO_3 ($\sim 0.3 < x < 2.0$) have been investigated with elastic and inelastic neutron scattering. Neutron diffraction studies of orthorhombic $D_{0.36}MoO_3$ show that deuterium is incorporated as -OD without any major structural change to the MoO_3 layer lattice. The inelastic neutron scattering spectra of H_xMoO_3 phases confirm that, for $H_{0.34}MoO_3$, H is present as —OH, but, for the monoclinic phases $H_{0.93}MoO_3$, $H_{1.68}MoO_3$ and $H_{2.0}MoO_3$, only peaks associated with $-OH_2$ groups are found.

Introduction

Reduction of MoO_3 in an aqueous acidic medium was shown by Glemser and Lutz (*1*) to lead to the formation of a series of oxide–hydroxide phases $MoO_{3-x}(OH)_x$ ($0.5 < x < 2.0$). The close resemblance of the powder X-ray patterns of the reduced phases (*2*) to that of MoO_3 suggested that hydrogen may readily be inserted into the parent oxide matrix with little crystallographic rearrangement (topotactic reduction). The results of a single crystal X-ray study of the first member of the series "$H_{0.5}MoO_3$" established (*3*) that the molybdenum–oxygen framework is substantially unchanged from that in MoO_3. The analogy between H_xMoO_3 and the well-known tungsten bronzes A_xWO_3 (*4*) formed by insertion of alkali metals and hydrogen into WO_3, is immediate. Unit cell parameters and approximate composition ranges of the phases H_xMoO_3 ($x \sim 0.3$, ~ 1.0, ~ 1.6, ~ 2.0) have recently been reported (*5*).

The object of the present work is the structural characterization of pure phases of hydrogen–molybdenum bronzes, H_xMoO_3, by means of powder neutron diffraction and inelastic neutron scattering.

Experimental Method

Materials

Pure phases of H_xMoO_3 were prepared following Glemser and Lutz (*1*). The most highly reduced phase, $H_{2.0}MoO_3$, was obtained by prolonged treatment of MoO_3 with Zn/HCl, whilst $H_{1.68}MoO_3$ was made by the dehydrogenation of $H_{2.0}MoO_3$ by heating at 110°C and 10^{-3} torr. $H_{0.93}MoO_3$ and $H_{0.34}MoO_3$ were made by treating mixtures of the more highly reduced phases with an aqueous slurry of MoO_3 in a sealed tube at 80°C. Manipulations were carried out in an oxygen-free atmosphere since all phases were sensitive to oxidation. Compositions of the bronzes were determined by ther-

0022-4596/79/050185-09$02.00/0

mogravimetry and by redox titrations. Resulting uncertainties in x were $\sim\pm0.02$.

Two samples of D_xMoO_3 ($x\sim0.36$) were prepared in sealed silica tubes at 80–90°C. Sample I was prepared from $MoO_3/Mo/D_2O$ whereas sample II was prepared from $MoO_3/D_{1.68}MoO_3/D_2O$, the $D_{1.68}MoO_3$ having been previously synthesised with DCl in the manner described above for the hydrogen material. Isotopically pure D_2O (Norsk. Hydro., 99.8% D) and DCl (Ciba, ~38% solution in D_2O, 99.5% D) were used. Both products were found to be of composition $D_{0.36+0.01}MoO_3$.

Powder X-Ray Diffraction

Guinier powder X-ray patterns of the pure phases MoO_3, $H_{0.34}MoO_3$ and $D_{0.36}MoO_3$ could be indexed on the basis of orthorhombic unit cells. The remaining phases could be indexed on the basis of monoclinic unit cells. The cell parameters (*5*) are shown in Table I.

Powder Neutron Diffraction

Neutron powder profiles were recorded on PANDA at A.E.R.E. Harwell in the range $8°<2\theta<105°$ in steps of 0.1°. The samples (~5 g) were contained in a thin-walled V can sealed with an In gasket. The profiles were recorded at room temperature (sample II) and at 4.2°K (sample I) using a liquid Helium cryostat. The neutron wavelengths of 1.5588 Å and 1.5375 Å respectively were obtained by reflection from the (511) planes of a Ge monochromator at a take-off angle of 90°.

Inelastic Neutron Scattering

Spectra were recorded at 80°K using the IN1B beryllium filter spectrometer at the I.L.L. Grenoble, an instrument similar to one which has been described previously (*6*). Incident neutrons were monochromated with the (200) (220) and (331) planes of a copper crystal. The samples were enclosed in silica tubes and the spectra in Figs. 4 and 5 have had the scattering contribution from the silica subtracted.

Results

The observed diffraction peaks from $D_{0.36}MoO_3$ were consistent with space groups *Cmcm*, $Cmc2_1$, and *C2cm*, as reported by previous workers (*2, 3*). They were analysed by the method of least-squares profile refinement (*8*) using initial halfwidth parameters and a zero-point correction determined manually. The initial atomic coordinates for Mo and O were those given by Wilhelmi (*3*) and the coherent neutron scattering lengths used were $b_{Mo}=0.69\times10^{-12}$, $b_O=0.58\times10^{-12}$ and $b_D=0.667\times10^{-12}$ cm (*9*).

Refinement was tried with deuterium atoms located in various sites both singly and in combinations and the best agreement was found for the intralayer positions between bridging oxygen atoms (Fig. 2). The interlayer positions between terminal oxygen atoms were clearly unsatisfactory giving

TABLE I

Phase	a, Å	b, Å	c, Å	α°
$H_{0.34}MoO_3$ (blue, orthorhombic)	3.896	14.07	3.736	90.0
$D_{0.36}MoO_3$ (blue, orthorhombic)	3.895	14.07	3.737	90.0
$H_{0.93}MoO_3$ (blue, monoclinic)	3.796	14.53	3.864	93.74
$H_{1.68}MoO_3$ (red, monoclinic)	3.770	13.97	4.055	93.97
$H_{2.0}MoO_3$ (green, monoclinic)	3.897	13.55	4.053	94.63
MoO_3 (*3*)	3.962	13.86	3.697	90.0

poorer agreement than a model with no deuterium atoms included. The refinement in *Cmcm* included seven positional and six thermal parameters, a preferred orientation parameter, the asymmetry parameter, the lattice constants, three peak halfwidth parameters, the zero-point correction and a scale-factor. During refinement with D in the 16(*h*) position, the deuterium *x* coordinate was observed to oscillate about 0.0 and was therefore constrained to this value, placing the deuterium atoms on the *yz* mirror plane in the 8(*f*) position. (No other satisfactory deuterium position was found.) Final refinement was accomplished using anisotropic thermal parameters for the deuterium atom, constrained such that $B_{11} = B_{33} \neq B_{22}$, $B_{12} = B_{13} = B_{23} = 0$. Fourier analyses, using the method described by Cheetham and Taylor (*9a*) carried out with and without inclusion of deuterium positions, showed no significant peaks other than those of Mo and O and a deuterium position at (0.0, 0.5, 0.5), midway between the statistically occupied sites that had been assumed. Refinements in $Cmc2_1$ and *C2cm* led to no significant improvement and *Cmcm* was taken as the actual space group. The final atomic coordinates are given in Table II and the agreement between the observed and calculated profiles is illustrated in Fig. 1 for the room temperature data. The room temperature and 4.2°K profiles were nearly identical.

The agreement factors, R_{profile}, defined by

$$R_{\text{profile}} = 100\sqrt{\frac{\Sigma_i w_i[\,y_i(\text{obs}) - Cy_i(\text{calc})]^2}{\Sigma_i w_i[\,y_i(\text{obs})]^2}}$$

converged to 12.48 for the room temperature data and 11.58 for the 4.2°K data. These values compare with 5.46 and 6.42 respectively, expected from purely statistical considerations. Values of $R_I = 100\Sigma|I(\text{obs}) - CI(\text{calc})|/\Sigma I(\text{obs})$ were 7.57 and 11.81 respectively.

TABLE II

ATOMIC COORDINATES FOR $D_{0.36}MoO_3$ at 4.2°K and 293°K. SPACE GROUP *Cmcm*

			4.2°K			
Atom		*x*	*y*	*z*	B Å^2	*n*
Mo	4(*c*)	0	0.1048(3)	$\frac{1}{4}$	0.71(8)	1.0
O1	4(*c*)	0	0.9328(3)	$\frac{1}{4}$	0.19(9)	1.0
O2	4(*c*)	0	0.5860(3)	$\frac{1}{4}$	0.47(9)	1.0
O3	4(*c*)	0	0.2234(3)	$\frac{1}{4}$	0.07(9)	1.0
D	8(*f*)	0	0.5257(22)	0.4352(111)		0.36
Anisotropic thermal parameters for atom D						
	B_{11}	B_{22}	B_{33}	B_{12}	B_{13}	B_{23}
	1.67(30)	0.74(55)	1.67(30)	0	0	0
			293°K			
Atom		*x*	*y*	*z*	B Å^2	*n*
Mo	4(*c*)	0	0.1041(3)	$\frac{1}{4}$	0.90(9)	1.0
O1	4(*c*)	0	0.9333(3)	$\frac{1}{4}$	0.47(10)	1.0
O2	4(*c*)	0	0.5857(4)	$\frac{1}{4}$	0.93(10)	1.0
O3	4(*c*)	0	0.2223(3)	$\frac{1}{4}$	0.86(11)	1.0
D	8(*f*)	0	0.5276(22)	0.4418(118)		0.36
Anisotropic thermal parameters for atom D						
	B_{11}	B_{22}	B_{33}	B_{12}	B_{13}	B_{23}
	2.00(30)	1.05(66)	2.00(30)	0	0	0

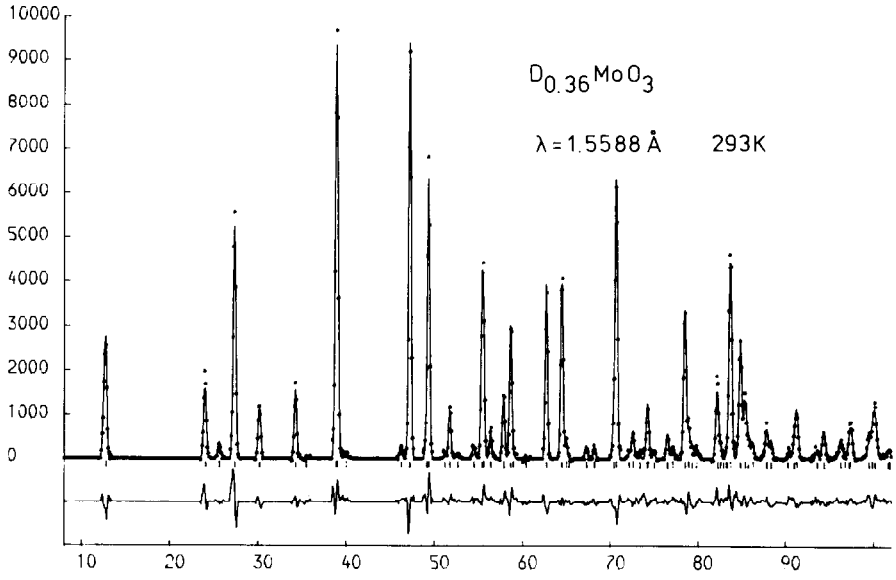

FIG. 1. Observed and calculated diffraction profiles for $D_{0.36}MoO_3$ at room temperature.

Discussion

The bond angles and atomic separations in the structure of $D_{0.36}MoO_3$, which are given in Table III, show reasonable agreement with the results of a single crystal X ray study (*3*).

A projection of the structure on (001) is shown in Fig. 2 together with the corresponding structure of MoO_3 (*7*). Further comparisons are shown in Fig. 3. As noted by Kihlborg (*7*), the coordination of Mo in MoO_3 is strongly distorted from octahedral and may be described in terms of a tetrahedral model with O2′ and O1 more distant than the nearest oxygen neighbours (4+2 coordination). The $D_{0.36}MoO_3$ structure comprises a more regular octahedral coordination (5+1) similar to that in $Mo_4O_{11.2}F_{0.8}$ (*10*).

The O2–O2″ distance of 3.05 Å contrasts with the OI–OII separation in H_xWO_3 of 3.26 Å (*11*). The deuterium atoms are statistically disordered between the O2 atoms and form deuteroxyl bonds so that a more

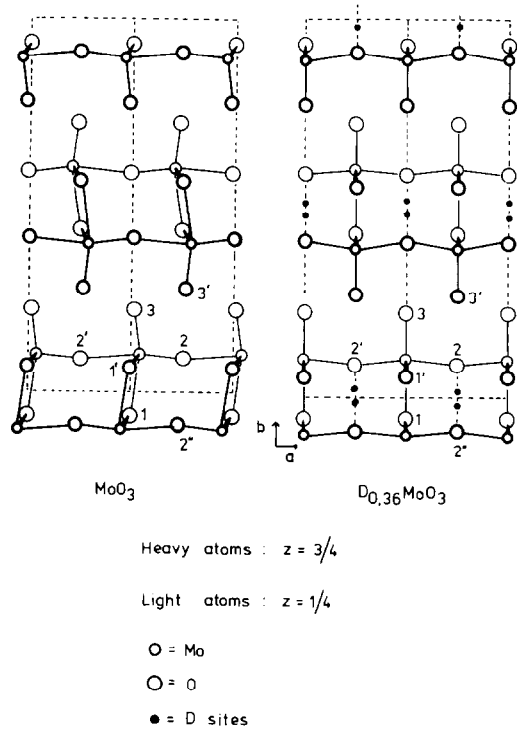

FIG. 2. Projections of the unit cells of $D_{0.36}MoO_3$ and MoO_3 onto the (001) plane.

TABLE III

INTERATOMIC DISTANCES AND ANGLES IN $D_{0.36}MoO_3$

Interatomic distances in MoO_6 octahedron (±0.006 Å)			
	4.2°K	~293°K	
Mo–O1	2.39	2.40	(2.33)
Mo–O1′ Mo–O1″[a]	1.94	1.94	(1.96)
Mo–O2 Mo–O2′	1.96	1.96	(1.96)
Mo–O3	1.65	1.66	(1.69)
O2–D[b]	1.09	1.09	
O2″–D	1.95	1.97	
O1′–D	2.34	2.33	

Angles (±0.5°)			
	4.2°K	293°K	
O1–Mo–O1′ O1–Mo–O1″	74	74	(73)
O1–Mo–O2 O1–Mo–O2′	82	82	(83)
O1′–Mo–O2 O1″–Mo–O2 O1′–Mo–O2′ O1″–Mo–O2′	88	88	(88)
O1′–Mo–O3 O1″–Mo–O3	106	106	(107)
O2–Mo–O3 O2′–Mo–O3	98	98	(97)
O2–D–O2″	178	175	

O–O distances (±0.006 Å)			
	4.2°K	~293°K	
O1–O1′ O1–O1″	2.64	2.65	(2.56)
O1–O2 O1–O2′	2.89	2.90	(2.86)
O1′–O2 O1′–O2′ O1–O2″ O1″–O2 O1″–O2′	2.71	2.71	(2.72)
O1′–O3 O1″–O3 O1–O3 O1–O3″[a]	2.87	2.88	(2.94)
O2–O3 O2′–O3	2.73	2.74	(2.74)
O2–O2″	3.04	3.05	(3.07)
O3–O3′	2.80	2.81	(2.80)

[a] O1″ = Reflection of O1′ about $z = \frac{1}{4}$.
O3″ = Inversion of O3 through origin.
[b] D = Deuterium closest to O2.
For key to atomic positions see Fig. 2.
Figures in parentheses are those of Wilhelmi (*3*).

informative formulation of the phase would be $MoO_{3-x}(OD)_x$ (cf. $WO_{3-x}(OH)_x$ (*11*)). The two sites between a pair of O2 atoms cannot be simultaneously occupied as this would involve D–D distances of ~1 Å. The calculated O–D bond-length of 1.09 at both room temperature and 4.2°K is reasonable in view of the large concentration of defects in the structure. The deuterium atoms are displaced from the O2–O2″ line with an angle O2–D–O2″ of 175° at 293°K. Proton NMR experiments on $H_{0.36}MoO_3$ (*12*) lead to a value for the second moment of ~5 g^2.[1] A calculation of this quantity based on random occupancy of the sites deduced from the neutron study (excluding simultaneous occupancy of adjacent sites ~1 Å apart) gives a value of 4.8 g^2 in fair agreement with experiment.

After the powder diffraction work described here was almost completed, it was

[1] This value has since been confirmed by Dr. B. G. Silbernagel of the Exxon Corporate Research Laboratories using a Varian WL-112 NMR spectrometer.

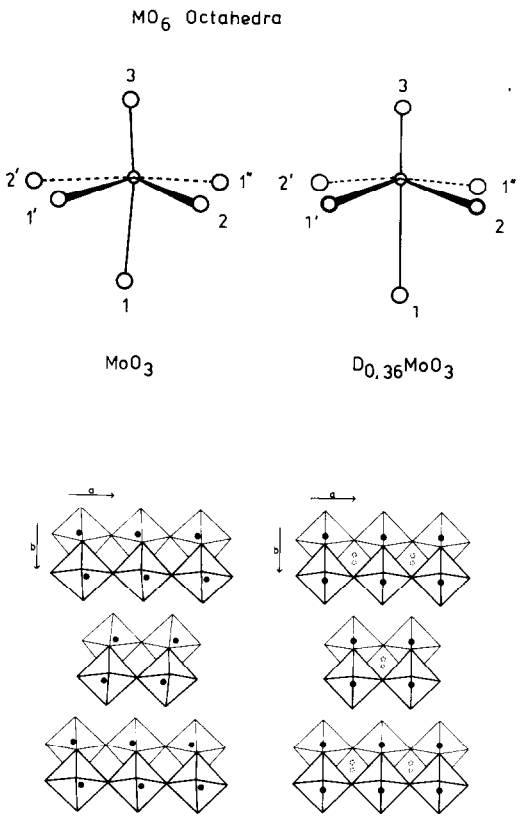

FIG. 3. Octahedral diagrams of $D_{0.36}MoO_3$ and MoO_3.

learned that a neutron profile study had been carried out on $H_{0.31}MoO_3$ (*13*). Reasonable agreement between the two studies is found although the H co-ordinates found in $H_{0.31}MoO_3$ (0.0, 0.461, 0.469) differ slightly from those given here and lead to an O–H bond length of 1.3 Å.

Complementary evidence for the occurrence of H as hydroxyl in $H_{0.34}MoO_3$ is provided by its inelastic neutron spectrum which in Fig. 4 is superimposed on the similar spectrum of the oxide–hydroxide $H_{0.4}WO_3$ (*14*). There is only one intense band at 1267 cm^{-1} in the central region of the spectrum which is compatible with the classification of this material as a hydroxide. The scattering at lower frequencies near 500 cm^{-1} is due to hydrogen atoms being carried with vibrating oxygen atoms in molybdenum oxygen bond stretching vibrations. The 1267 cm^{-1} excitation due to the Mo–O–H deformation vibration is higher in energy than the corresponding excitation in $H_{0.4}WO_3$ at 1146 cm^{-1}.

The inelastic neutron scattering spectra of phases with higher hydrogen contents are shown in Fig. 5 and the positions of the major peaks in each spectrum are recorded in

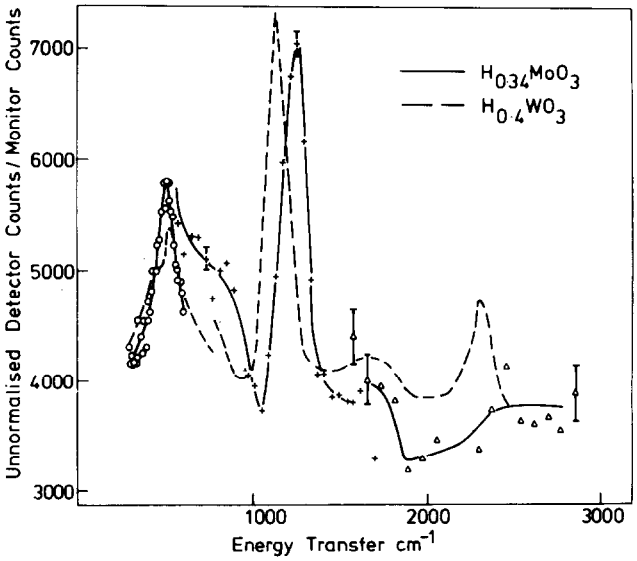

FIG. 4. Inelastic neutron spectra of $H_{0.4}WO_3$ and $H_{0.34}MoO_3$ (OOOO, ++++, and △△△△ refer to neutrons monochromated by 200, 220 and 331 planes respectively).

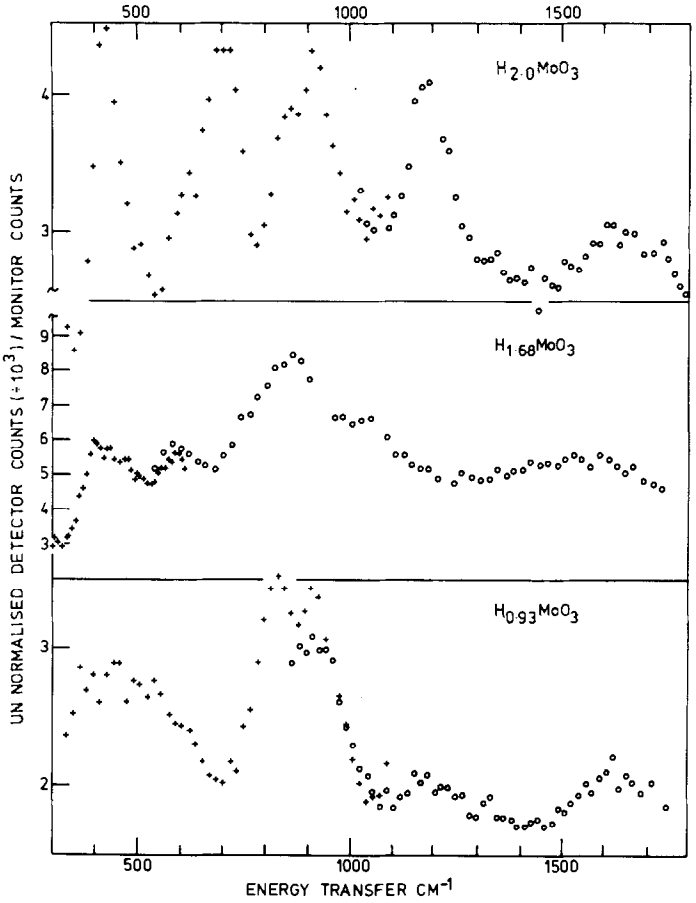

FIG. 5. Inelastic neutron spectra of $H_{0.93}MoO_3$, $H_{1.68}MoO_3$ and $H_{2.0}MoO_3$ (++++ and OOOO refer to neutrons monochromated by 200 and 220 planes respectively). (Further data up to 2900 cm^{-1} for $H_{1.68}MoO_3$ reveal no additional features).

Table IV. The spectra are more complex than that of $H_{0.34}MoO_3$ but the occurrence of scattering in the region of 1600 cm^{-1}, where the H–O–H deformation vibration of an OH_2 group is found, implies that all the higher phases contain these units.

At lower frequencies it is anticipated that scattering from the torsional oscillations of the OH_2 groups will lead to further peaks in the neutron spectrum. The experimental spectrum for ice (*17*), for example, shows the presence of two peaks at 600 and 808 cm^{-1}. For H_xMoO_3 above 800 cm^{-1}, little scattering is found for the lowest phase (apart from the M–O–H deformation), but for the remaining phases two new bands appear in the range 800–1200 cm^{-1} which increase uniformly in frequency with increasing hydrogen content. These bands may tentatively be assigned to OH_2 torsional oscillations. The increase in frequency with hydrogen content parallels the simultaneous lattice contraction (Fig. 6). In Fig. 6 a correlation diagram is plotted linking vibrations of a likely common origin in the various phases. In the construction of this diagram it has been assumed that the M–O framework vibrations, which lead to significant displacements of H atoms, are confined to the region below 800 cm^{-1} as was found to be so for $H_{0.4}WO_3$ and $H_{0.34}MoO_3$.

TABLE IV

MEASURED VIBRATION FREQUENCIES (cm^{-1}) IN H_xMoO_3

$H_{0.4}WO_3$	$H_{0.34}MoO_3$	$H_{0.93}MoO_3$	$H_{1.68}MoO_3$	$H_{2.0}MoO_3$
		395[a]		
428		452[a]	396	428
541	517	541[a]	593	621 (w)
	823	626[a]		702
				872 (Sh)
		823	864	920
		912	1045	1186
1146	1267	1186 (w)		
		1670	1574	1622

[a] Frequencies taken from a spectrum with higher resolution and statistical accuracy than that shown in Fig. 5. (w) weak, (Sh) shoulder.

The correlation diagram suggests that for the monoclinic phases H_xMoO_3 ($x = 0.93$, 1.68, 2.0) a progressive structural change influences the vibrations of similarly situated hydrogen atoms. The formation of new hydrogen sites is unlikely because at no point does the number of intense bands in the spectrum increase. It is suggested that all the protons in the monoclinic phases are present in OH_2 groups in one location, probably between the layers. For example, a model involving two hydrogen atoms bonded to each O3 atom with O–H bonds directed towards O2 atoms of the adjoining layer is compatible with the neutron spectrum. Alternative models involving occupation of both inter- and intralayer positions by protons would be expected to give a larger number of bands unless accidental degeneracy occurred.

The above conclusions interpret the most intense bands in the spectra, but there is also a weak band at $\sim 1200\ cm^{-1}$ in $H_{0.93}MoO_3$ which could be due to a small quantity of

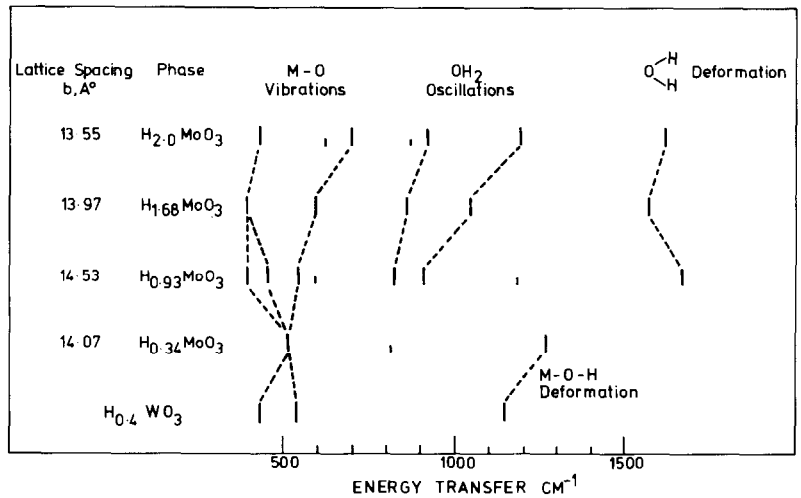

FIG. 6. Correlations between the vibrations of H_xMoO_3 and $H_{0.4}WO_3$ (long and short lines correspond approximately to the relative intensities).

hydroxyl groups present in this phase. Apart from this there is no evidence for any large concentration of hydroxyl groups, of the type present in $H_{0.4}WO_3$ and $H_{0.34}MoO_3$, in the phases of higher hydrogen content.

Contributions to neutron spectra can arise from the scattering of higher harmonics of simple oscillators, and this scattering has been shown to be very important in the cases of $H_{0.4}WO_3$ and H_xTaS_2 (*18*). In those cases the scattering is well described as that from a single local oscillator of effective mass 1. For oscillators of higher effective masses which will arise from vibrational mixing of hydrogen and oxygen vibrations, scattering from harmonics will be much reduced, and this appears to be the case for the molybdenum oxide phases of hydrogen concentration >0.34. In $H_{1.68}MoO_3$ there is no appreciable scattering at twice the energy transfer of the vibration at 864 cm^{-1}.

Conclusion

Diffraction and inelastic scattering studies show that the protons in $H_{0.34}MoO_3$ are present as hydroxyl groups which can be only weakly hydrogen bonded. In the phases with higher concentrations of protons the scattering data show that OH_2 groups are formed and in addition suggest that in all three phases all the protons are present in such groups.

Acknowledgments

The authors thank the S.R.C. for providing neutron beam facilities and a Research Studentship for one of us (J.J.B.). Computational assistance from D. J. Palmer is gratefully acknowledged.

References

1. O. GLEMSER AND G. LUTZ, *Z. Anorg. Allg. Chem.* **264**, 17 (1951).
2. L. KIHLBORG, G. HÄGERSTRÖM, AND A. RONNQUIST, *Acta Chem. Scand.* **15**, 1187 (1961).
3. K.-A. WILHELMI, *Acta Chem. Scand.* **23**, 419 (1969).
4. P. G. DICKENS AND P. J. WISEMAN, *Oxide Bronzes*, M.T.P. International Review of Science, Series Two, *Inorg. Chem.* **10**, 211, (1975).
5. J. J. BIRTILL AND P. G. DICKENS, *Mater. Res. Bull.* **13**, 311 (1978).
6. M. F. COLLINS, B. C. HAYWOOD, AND G. C. STIRLING, *Disc. Farad. Soc.* **48**, 163 (1969).
7. L. KIHLBORG, *Ark. Kemi* **21**, 357 (1963).
8. H. M. RIETVELD, *J. Appl. Crystallogr.* **2**, 65 (1969).
9. G. E. BACON, *Acta Crystallogr. A* **28**, 357 (1972).
9a. A. K. CHEETHAM AND J. C. TAYLOR, *J. Solid State Chem.* **21**, 253 (1977).
10 J. W. PIERCE, M. VLASSE, AND A. WOLD, *Acta Crystallogr. B* **27**, 158 (1971).
11. P. J. WISEMAN AND P. G. DICKENS, *J. Solid State Chem.* **6**, 374 (1973).
12. P. C. T. SLADE AND T. K. HALSTEAD, to be published.
13. F. SCHRODER AND H. WEITZEL, *Z. Anorg. Allg. Chem.* to be published.
14. C. J. WRIGHT, *J. Solid State Chem.* **20**, 89 (1977).
15. H. L. KRAUSS AND W. HUBER. *Chem. Ber.* **94**, 2864 (1961).
16. J. R. GUNTER, *J. Solid State Chem.* **5**, 354 (1971).
17. J. HOWARD, T. C. WADDINGTON, AND C. J. WRIGHT. Conf. on Inel. Neutron Scattering, Vol. II, p. 499, I.A.E.A., Vienna, 1977.
18. C. J. WRIGHT, C. RIEKEL, R. SCHOLLHÖRN, AND B. C. TOFIELD. *J. Solid State Chem.* **24**, 219 (1978).